# Next-generation all-solid-state battery (#ASSB)

Tuan Vo<sup>a,b†</sup>, Claas Hüter<sup>b</sup>, Stefanie Braun<sup>a</sup>, Manuel Torrilhon<sup>a</sup>

<sup>a</sup>Department of Mathematics, Applied and Computational Mathematics (ACoM), RWTH Aachen University, Schinkelstraße 02, 52062 Aachen, Germany 
<sup>b</sup>Institute of Energy and Climate Research (IEK-2), Forschungszentrum Jülich, Wilhelm-Johnen-Straße, 52428 Jülich, Germany

### Mathematical modelling for the next-generation All-solid-state batteries: Nucleation $(SE|SSE)^{(*)}$ -interface

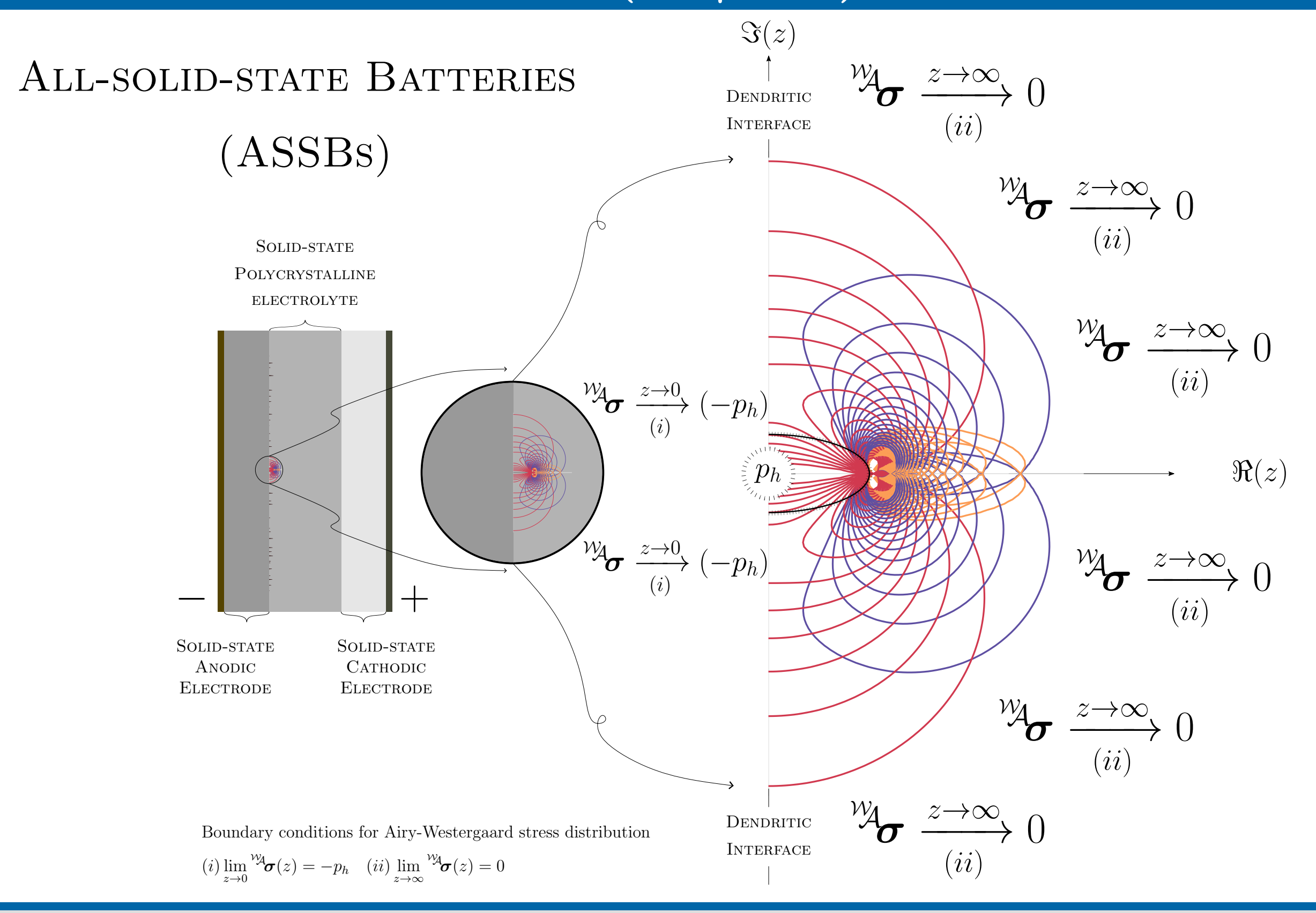
Rechargeable Lithium-ion battery (LIB) is at the heart of every electric vehicle (EV), portable electronic device, and energy storage system [1]. Nowadays, LIBs enable human life more efficient and help to solve global environment issues thanks to EVs' zero emission. However, conventional LIB (c-LIB) is sensible to temperature and pressure, hence, flammable and explosive, which is undesirable. This bottleneck is mainly due to liquid-based electrolyte found in c-LIBs.

All-solid-state battery (ASSB) is one of promising candidates to overcome bottlenecks of c-LIBs. Thanks to solid-state electrolyte (SSE), ASSB is highly stable towards temperature and pressure. Nevertheless, Limetal dendrite triggered at (SE|SSE)-interface [5] is the main drawback of ASSB since these dendritic threads extrapolate into SSE grain boundary network, causing crevice, degradation of ionic conductivity, and the probability of short-circuit, which is unfavorable.

Next-generation All-solid-state battery (ng-ASSB) with a consideration of nucleation criterion defined by

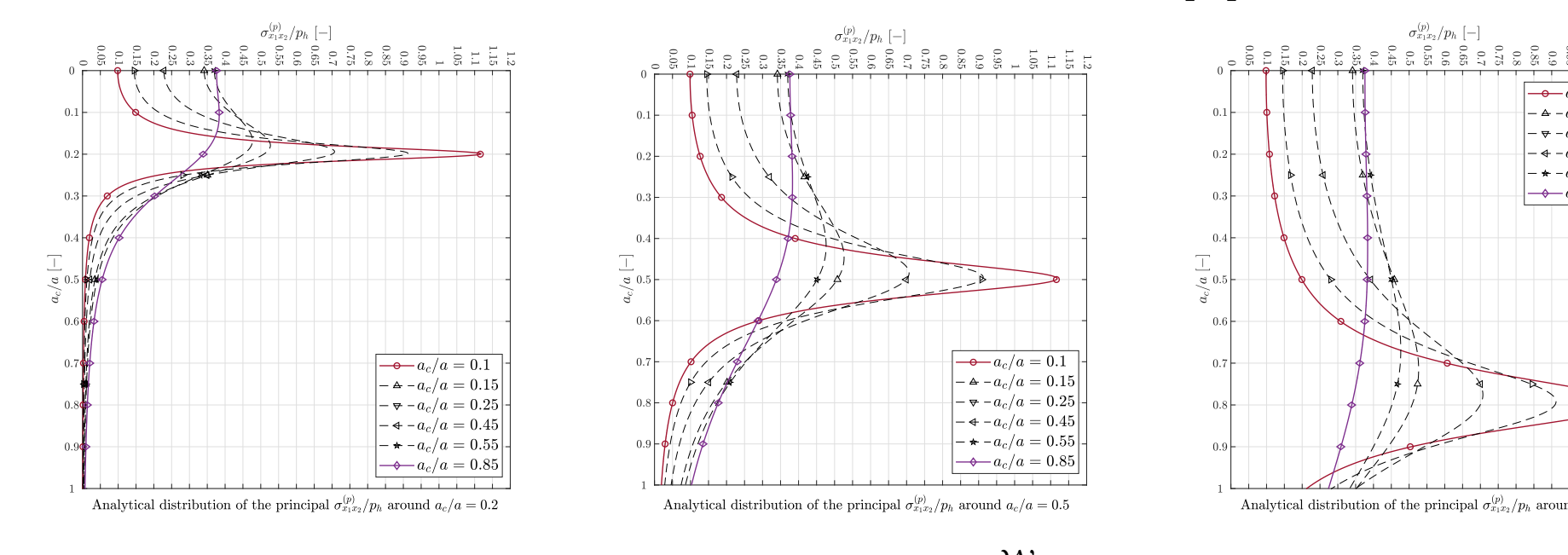
$$a_{\text{Griffith}} := a^* = \arg\min_{a \in \mathbb{R}} \left. \iint_{\Omega} f(a, \boldsymbol{u}, \boldsymbol{\theta}; \lambda, \mu, \boldsymbol{d}^R \otimes \boldsymbol{d}^R) \, d\Omega - \left. \iint_{\Gamma} f(a; \gamma) \, d\Gamma \right|_{\boldsymbol{u}^{(s)}}$$

where  $\boldsymbol{u}$  displacement field,  $\theta$  temperature field, a crevice length,  $\lambda$ ,  $\mu$  Lamé constants,  $\boldsymbol{d}^R \otimes \boldsymbol{d}^R$  embedded misorientation structural tensor, and  $\gamma$  cracking-surface energy density, can help to improve ASSB performance.



### Interface Analysis

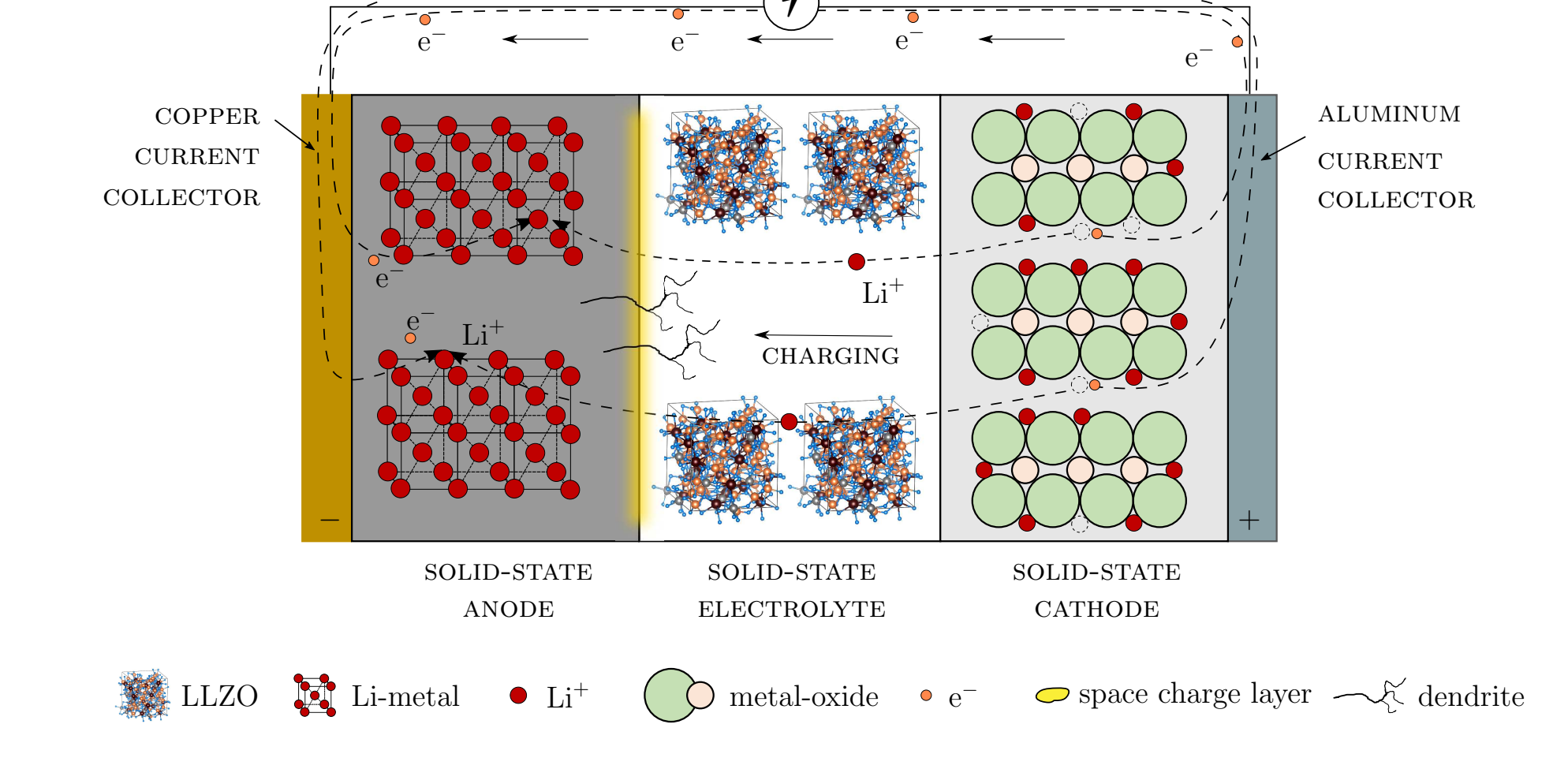
Interface between solid electrode and solid-state electrolyte (SE|SSE) taking place at space charge layer (SCL) [2] found in ASSBs critically exhibits mechanical and electrochemical instability [3]. This evidence points directly to the fact that the soft metallic li anode is erroneously prone to triggering dendrites, under cycles of electric charge & discharge [5].



<u>Distribution</u>: ana. max. shear stress  ${}^{\mathcal{V}}\!\!\sigma_{x_1x_2}^{\Pi}$  around crack tip  $a_c$ .

### Next-generation All-solid-state battery

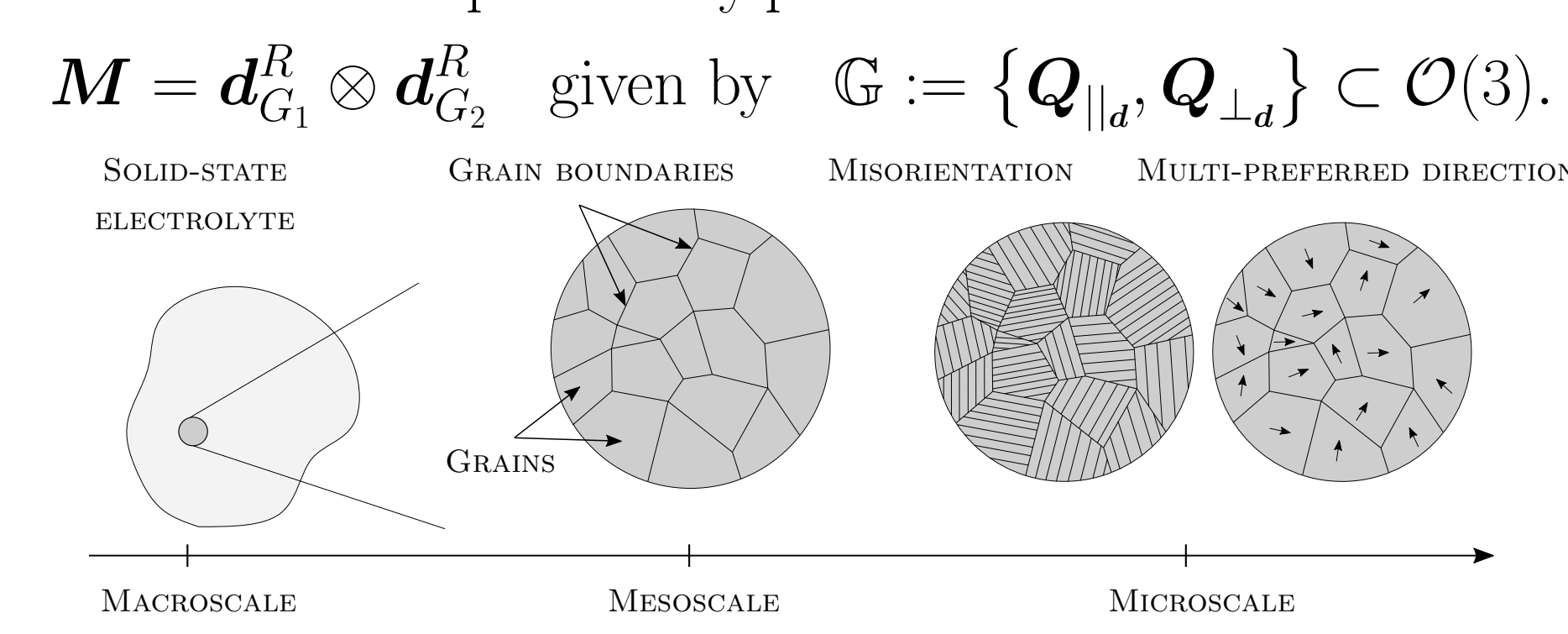
**Nucleation** criterion governs the instable (SE|SSE)-interface [3]



✓ **Thermodynamic consistency** is satisfied, followed by [2]. ✓ **Closure**  $\bar{\Omega}$  is fulfilled by 15 moments, followed by [4].

### Embedded structural-tensor in SSE

**Polycrystalline** garnet-type SSE [5] such as LLZO exhibit grain boundary network, and grains with variation of {size, shape} under microscopic observation. Hence, this microstructure is potentially prone to nuances of destruction.



Consequentially, dendrites contribute to degradation of ionic conductivity and tiny-cracks tracing along grain boundaries.

### Nucleation interface: Taking place at the critical dendritic interface

Coupled fields: Displacement field  $\boldsymbol{u}$  and temperature field  $\boldsymbol{\theta}$ ; structural tensor  $\boldsymbol{M}$ 

$$\boldsymbol{u}: \begin{cases} \Omega \times \mathbb{R}_{+} \to \mathbb{R}^{3}, \\ (\boldsymbol{x},t) \mapsto \boldsymbol{u}(\boldsymbol{x},t), \end{cases} \quad \theta: \begin{cases} \Omega \times \mathbb{R}_{+} \to \mathbb{R}, \\ (\boldsymbol{x},t) \mapsto \theta(\boldsymbol{x},t), \end{cases} \quad \boldsymbol{M}_{i=1,\dots,N}^{\{RR,RE\}}: \begin{cases} \boldsymbol{d}_{\text{Grain i}}^{R} \otimes \boldsymbol{d}_{\text{Grain i}}^{R} \\ \boldsymbol{d}_{\text{Grain i}}^{R} \otimes \boldsymbol{d}^{E} \end{cases}$$

Governing conservation equations

$$\frac{d}{dt} \int_{\Omega} (\cdot) \ d\Omega = \int_{\Omega} (\cdot)^{\text{action}} \ d\Omega + \int_{\partial \Omega} (\cdot)^{\text{action}} \ d\partial\Omega + \int_{\Omega} (\cdot)^{\text{production (+/-)}} \ d\Omega$$

used to describe balance of mass, conservation of linear momentum, conservation of angular momentum, and conservation of energy with  $\rho(\boldsymbol{x},t)$  is mass density per unit volume (puv);  $\boldsymbol{b}(\boldsymbol{x},t)$  body force puv;  $\boldsymbol{v}(\boldsymbol{x},t)$  velocity;  $e(\boldsymbol{x},t)$  internal energy puv;  $\boldsymbol{q}(\boldsymbol{x},t)$  heat flux;  $r(\boldsymbol{x},t)$  heat source puv;  $\boldsymbol{\sigma}$  Cauchy stress and  $\boldsymbol{\varepsilon}$  infinitesimal strain. Then, the governing partial differential equation (PDE) of deformation takes the form

$$\partial_t oldsymbol{u} + 
abla \cdot \left( \overset{4}{\mathbb{C}}^{f_{ ext{alocation}}(\lambda, \mu, oldsymbol{d}_{G_i, i=1,...,N}^R, oldsymbol{d}^E; oldsymbol{x})} : 
abla oldsymbol{u}^{(s)} 
ight) + 
ho oldsymbol{b} = -
ho 
abla V_e,$$

where  $V_e : \mathbb{R}^3 \to \mathbb{R}$  is the electric potential applied globally on ASSB. Due to nature setting of ASSB taking the form (SE|SSE|SE) the electric potential becomes uniform.

**Strain energy** is based on the deformation of SSE due to dendrite formation at (SE|SSE)-interface

 $\iiint_{\Omega} f(a, \boldsymbol{u}; \lambda, \mu, \boldsymbol{d} \otimes \boldsymbol{d}) d\Omega$ 

Surface energy is analysized based on the open crevice cracking at (SE|SSE)interface affected by prescribed pressure

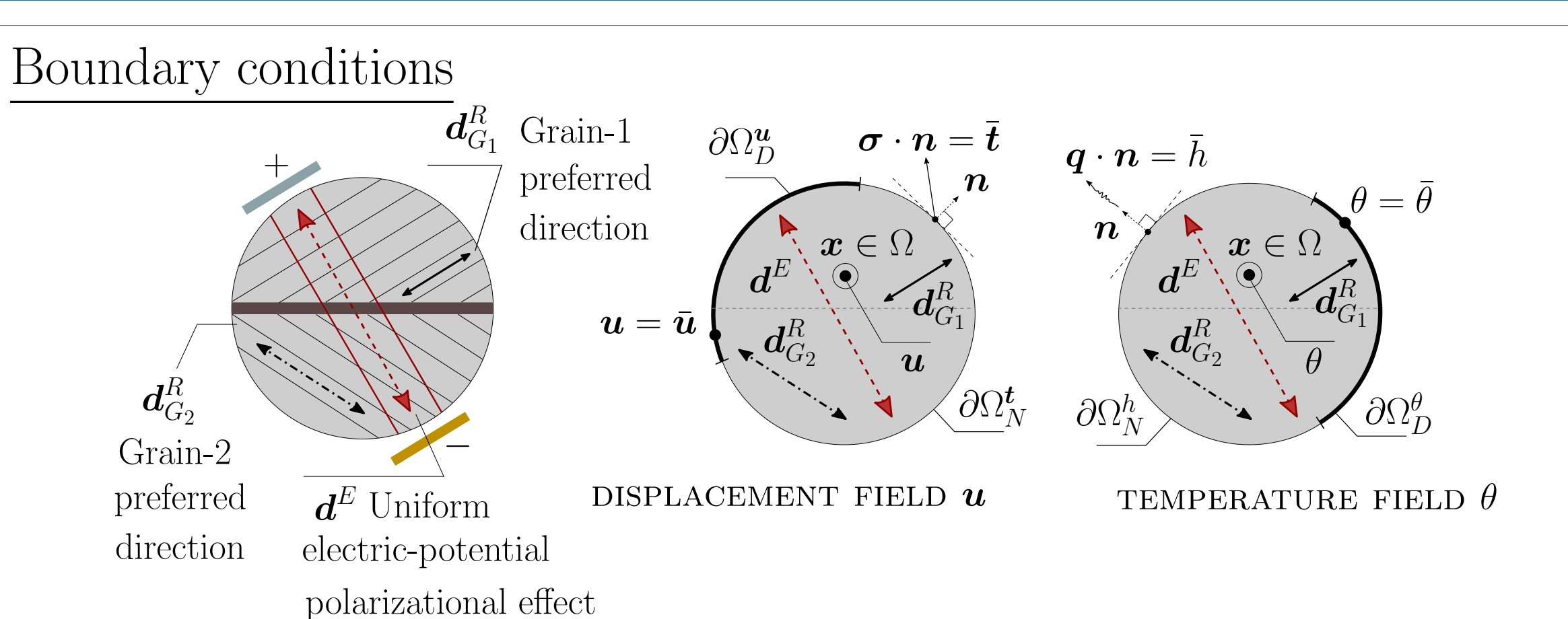
$$\iint_{\Gamma} f(a;\gamma) \, d\Gamma$$

Therefore, the governing problem of dendritic nucleation at (SE|SSE) takes the form

$$\partial_{t}\boldsymbol{u} + \nabla \cdot \left( \mathbb{C}^{f_{\text{alocation}}(\lambda, \mu, \boldsymbol{d}_{G_{i}, i=1,\dots,N}^{R}, \boldsymbol{d}^{E}; \boldsymbol{x})} : \nabla \boldsymbol{u}^{(s)} \right) + \rho \boldsymbol{b} = -\rho \nabla V_{e}, \tag{1}$$

s.t. 
$$a_{\text{Griffith}} := a^* = \arg\min_{a \in \mathbb{R}} \iiint_{\Omega} f(a, \boldsymbol{u}, \theta; \lambda, \mu, \boldsymbol{d} \otimes \boldsymbol{d}) d\Omega - \iint_{\Gamma} f(a; \gamma) d\Gamma \Big|_{\bar{\boldsymbol{u}}}$$
 (2)

where deformation  $\bar{\boldsymbol{u}}$  is (i) based on (1), and then (ii) for Griffith-analysis in (2).



Numerical spectral of Griffith criterion in x-direction at (SE|SSE) yields a = 0.05 (c) Case 3 (d) Case 4 (e) Case 5  $a_{crevice} = 0.05$ 

where a sample of 5 cases with various prescribed crevice length is studied.

FEM: Strain energy density

Partial differential equation (PDE)  $\nabla \cdot \begin{pmatrix} \frac{4}{C} f^{\mathbb{D}(\Omega)} \\ \nabla^{(s)} u \end{pmatrix} + \rho \, \boldsymbol{b} = \boldsymbol{0}$ Displacement vector field solution  $\boldsymbol{u_i} \leftarrow \boldsymbol{u} = \boldsymbol{K}^{-1} \boldsymbol{f}$ Strain tensor  $\varepsilon_{ij} = \frac{1}{2} \left( \partial_{x_j} \boldsymbol{u_i} + \partial_{x_i} \boldsymbol{u_j} \right)$ Stress tensor  $\boldsymbol{\sigma_{ij}} = \sum_{k,l} \overset{4}{C} f^{\mathbb{D}(\Omega)}_{(\lambda,\mu)} \varepsilon_{kl}$ Strain energy density  $\mathcal{E}_{\text{strain}} := \frac{1}{2} \sum_{i,j} \boldsymbol{\sigma_{ij}} \varepsilon_{ij}$ Strain solution takes the following form  $\frac{1}{2} \sum_{\alpha=1}^{N\Omega^e} \overset{N\Omega^{\text{node}}}{C} \overset{N\Omega^{\text{node}}}{C}} \overset{N\Omega^{\text{node}}}{C} \overset{N$ 

Analysis: Airy-Westergaard function used for stress analysis: (i) max. shear stress and (ii) principal stresses

$$\mathcal{A}: \begin{cases} \mathbb{C} \to \mathbb{C}, \\ z \mapsto \mathcal{V} \mathcal{A}(z) := \Re(\iint_{\Gamma} \mathcal{K}^{(\star)} dz) + x_2 \Im(\oint_{\Gamma} \mathcal{K}^{(\star)} dz), \end{cases} \mathcal{K}^{(\star)}: \begin{cases} \mathbb{C} \to \mathbb{C}, \\ z \mapsto \mathcal{K}^{(\star)} := -p_h + p_h/\sqrt{1 - a^2/z^2}, \end{cases}$$

where a the crevice length,  $p_h$  pressure at the opening crevice on dendritic interface, and  $\forall \{p_h, a\} \in \mathbb{R}_+$ .

Numerics  $\to$  FEM: element matrix  $\boldsymbol{K}^{e}$  approx. by  $Gauss\ quadrature$ ; indices imply 4+2=6 for-loop:  $K_{ik}^{e^{\alpha\beta}} = \int_{\Omega^{\xi}} \left( \mathcal{L}_{1}^{\alpha} \, \mathbb{C}_{i1k1}^{f^{GL}}(\boldsymbol{x}) \, \mathcal{R}_{1}^{\beta} + \mathcal{L}_{1}^{\alpha} \, \mathbb{C}_{i1k2}^{f^{GL}}(\boldsymbol{x}) \, \mathcal{R}_{2}^{\beta} + \mathcal{L}_{2}^{\alpha} \, \mathbb{C}_{i2k1}^{f^{GL}}(\boldsymbol{x}) \, \mathcal{R}_{1}^{\beta} + \mathcal{L}_{2}^{\alpha} \, \mathbb{C}_{i2k2}^{f^{GL}}(\boldsymbol{x}) \, \mathcal{R}_{2}^{\beta} \right) \det(\boldsymbol{J}) \, d\Omega^{\xi}$ 

where  $\mathcal{L}_i^{\alpha}$  and  $\mathcal{R}_l^{\beta}$  are gradients of basis functions at node  $\alpha^{th}$  and  $\beta^{th}$ , respectively.

#### Contact

Tuan Vo vo@acom.rwth-aachen.de



## References

[1] T.Vo, Modeling the swelling phenomena of li-ion batt. cells based on a numerical chemo-mech. coupled approach. MA, Robert Bosch Battery Systems GmbH, 2018.

[2] **S.Braun**, C.Yada and A.Latz, Thermodynamically consistent model for Space-Charge-Layer formation in a solid electrolyte. Jr. Phys. Chem., 119, 22281-22288, **2015**. [3] **C.Hüter**, S.Fu, M.Finsterbusch, E.Figgemeier, L.Wells, and R.Spatschek, Electrode-electrolyte interface stability in solid state electrolyte system: influence of coating thickness under varying residual stresses. AIMS Materials Science, 4(4):867-877, **2017**.

[4] **M.Torrilhon**. Modeling nonequilibrium gas flow based on moment equations. Annual Review of Fluid Mechanics, 48(1):429-458, **2016**.

[5] **S.Kim**, J.S.Kim, L.Miara, Y.Wang, S.K.Jung, S.Y.Park, Z.Song, H.King, M.Badding, J.M.Chang, V.Roev, G.Yoon, R.Kim, J.H.Kim, K.Yoon, D.Im, and K.Kang, High-energy and durable li metal batt. using garnet-type solid electrolytes with tailored li-metal compatibility. Nature Communications, 13(1):1883, **2022**.









